

AD-A168 013

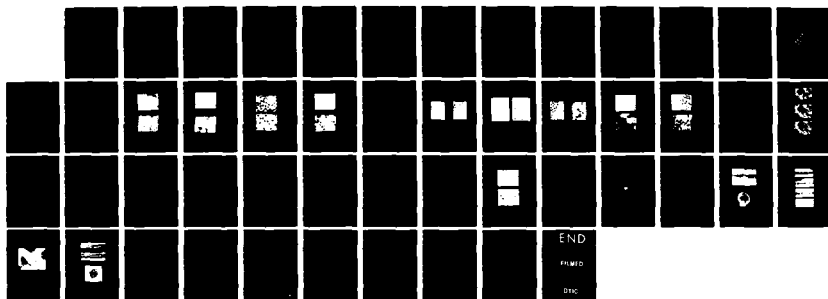
MESOPHASE BEHAVIOR FUNDAMENTAL TO PROCESSING OF  
CARBON-CARBON COMPOSITES. (U) AEROSPACE CORP EL SEGUNDO  
CA MATERIALS SCIENCES LAB J L WHITE ET AL. DEC 83  
TR-0084(4728-01)-2 SD-TR-85-38

171

UNCLASSIFIED

F/G 11/4

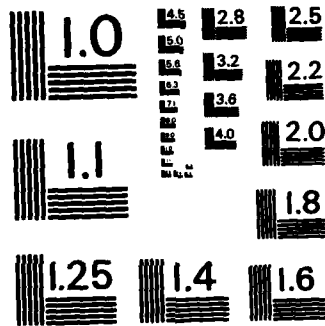
NL



END

FILMED

DTC



MICROCOPY RESOLUTION TEST CHART  
NATIONAL BUREAU OF STANDARDS-1963-A

12

REPORT SD-TR-85-38

Contract No. N00014-81-MP0006; NR-039-183

AD-A160 013

## Mesophase Behavior Fundamental to the Processing of Carbon-Carbon Composites

J. L. WHITE and P. M. SHEAFFER  
Materials Sciences Laboratory  
The Aerospace Corporation  
El Segundo, CA 90245

December 1983

Interim Technical Report for  
Period 1 October 1982 through 30 September 1983

APPROVED FOR PUBLIC RELEASE; DISTRIBUTION UNLIMITED

DTIC FILE COPY

DTIC  
ELECTE  
OCT 11 1985  
S E D

Prepared for  
OFFICE OF NAVAL RESEARCH  
800 North Quincy Street  
Arlington, VA 22217  
SPACE DIVISION  
AIR FORCE SYSTEMS COMMAND  
Los Angeles Air Force Station  
P.O. Box 92960, Worldway Postal Center  
Los Angeles, CA 90009-2960

85 10 11 020

This report was submitted by The Aerospace Corporation, El Segundo, CA 90245, under Contract No. F04701-83-C-0084 with the Space Division, P.O. Box 92960, Worldway Postal Center, Los Angeles, CA 90009-2960. It was reviewed and approved for The Aerospace Corporation by L. R. McCreight, Director, Materials Sciences Laboratory. First Lieutenant Brian Berliner, SD/YXM, was the Air Force project officer.

This report has been reviewed by the Public Affairs Office (PAS) and is releasable to the National Technical Information Service (NTIS). At NTIS, it will be available to the general public, including foreign nationals.

This technical report has been reviewed and is approved for publication. Publication of this report does not constitute Air Force approval of the report's findings or conclusions. It is published only for the exchange and stimulation of ideas.



Brian Berliner, 1Lt, USAF  
Project Officer, SD/YXM



Joseph Hess, GM-15  
Director, AFSTC West Coast Office  
AFSTC/WCO OL-AB

UNCLASSIFIED

SECURITY CLASSIFICATION OF THIS PAGE (When Data Entered)

| REPORT DOCUMENTATION PAGE   |   | READ INSTRUCTIONS<br>BEFORE COMPLETING FORM   |
|---|---|---|
| 1. REPORT NUMBER<br>SD-TR-85-38   | 2. GOVT ACCESSION NO.<br><b>AD-A160 013</b> | 3. RECIPIENT'S CATALOG NUMBER   |
| 4. TITLE (and Subtitle)<br><br>MESOPHASE BEHAVIOR FUNDAMENTAL TO THE<br>PROCESSING OF CARBON-CARBON COMPOSITES  |   | 5. TYPE OF REPORT & PERIOD COVERED<br>Interim Technical Report<br>1 Oct. 1982-30 Sept. 1983 |
| 7. AUTHOR(s)<br><br>J. L. White and P. M. Sheaffer  |   | 6. PERFORMING ORG. REPORT NUMBER<br>TR-0084(4728-01)-2                                      |
| 9. PERFORMING ORGANIZATION NAME AND ADDRESS<br>Materials Sciences Laboratory<br>The Aerospace Corporation<br>El Segundo, California 90245   |   | 8. CONTRACT OR GRANT NUMBER(s)<br>N00014-81-MP0006<br>NR 039-183;<br>F04701-83-C-0084       |
| 11. CONTROLLING OFFICE NAME AND ADDRESS<br>Office of Naval Research<br>800 North Quincy Street<br>Arlington, Virginia 22217   |   | 10. PROGRAM ELEMENT, PROJECT, TASK<br>AREA & WORK UNIT NUMBERS                              |
| 14. MONITORING AGENCY NAME & ADDRESS (if different from Controlling Office)<br>Space Division<br>Los Angeles Air Force Station<br>Los Angeles, California 90009-2960  |   | 12. REPORT DATE<br>December 1983  |
|   |   | 13. NUMBER OF PAGES<br>44   |
|   |   | 15. SECURITY CLASS. (of this report)<br><br>Unclassified                                    |
|   |   | 15a. DECLASSIFICATION/DOWNGRADING<br>SCHEDULE   |
| 16. DISTRIBUTION STATEMENT (of this Report)<br><br>Approved for public release; distribution unlimited.   |   |   |
| 17. DISTRIBUTION STATEMENT (of the abstract entered in Block 20, if different from Report)  |   |   |
| 18. SUPPLEMENTARY NOTES<br><br>cont'd   |   |   |
| 19. KEY WORDS (Continue on reverse side if necessary and identify by block number)<br>Carbon-carbon composite      Pyrolysis<br>Carbon fiber,      Wetting,<br>Petroleum pitch,      Disclination,<br>Coal-tar pitch,      Liquid crystal<br>Carbonaceous mesophase   |   |   |
| 20. ABSTRACT (Continue on reverse side if necessary and identify by block number)<br>The behavior of the carbonaceous mesophase under composite-fabrication conditions is being investigated to ascertain (1) how microstructure forms within the fiber matrix, (2) which mechanisms determine process efficiency, and (3) the ways in which carbonizing and graphitizing heat treatments affect matrix properties. This second annual report summarizes microstructural findings on impregnated fiber bundles quenched from various states of pyrolysis and describes the application of a penetrometric test to determine |   |   |

DD FORM 1473  
(FACSIMILE)

UNCLASSIFIED

SECURITY CLASSIFICATION OF THIS PAGE (When Data Entered)

UNCLASSIFIED

SECURITY CLASSIFICATION OF THIS PAGE (When Data Entered)

19. KEY WORDS (Continued)

20. ABSTRACT (Continued)

the pyrolysis conditions required to harden the mesophase. Also described are methods of extrusion and draw to prepare mesophase rods of well-defined microstructure, which are required to study the effects of heat treatment on dimensions, thermal expansivity, and the mechanical properties of the mesophase microconstituents in the composite. Originator supplied

Key words include:

Mesophase Formation within Fiber Bundles. Observations were made on specimens consisting of a fiber (one of four types) and a pitch matrix (either A240 petroleum pitch or 15V coal-tar pitch). They revealed some aspects of the patterns of mesophase formation within fiber bundles to be remarkably similar to each other and to differ from those observed in bulk pyrolysis. Both pitch and mesophase wet the filaments, and the pitch-mesophase interfacial energy is low relative to the surface energies of pitch or mesophase. Bloating caused by pyrolysis-gas-bubble growth and nucleation appears to have little effect on matrix microstructures. The tendency of mesophase to align on the filament surfaces—the "sheath" effect—dominates as the determining mechanism in forming matrix microstructure within a fiber bundle.

Mesophase Hardening. Applying a temperature-programmed penetrometer test to mesophase specimens prepared from A240 petroleum pitch and 15V coal-tar pitch indicated that the coal-tar pitch requires slightly more severe pyrolysis conditions for hardening. In room-pressure pyrolysis at 5°C/hr, both systems were fully hardened by pyrolysis to 476°C.

Mesophase Specimens of Well-defined Microstructure. Mesophase rods with fine fibrous microstructures were prepared by extrusion and draw methods similar to those used in the spinning of mesophase carbon fiber. Draw was demonstrated to be more effective than extrusion in attaining strong preferred orientations. The presence of gas bubbles in the extrudate constitutes the most serious obstacle to the preparation of highly oriented reproducible specimens.

UNCLASSIFIED

SECURITY CLASSIFICATION OF THIS PAGE (When Data Entered)

# PREFACE

This is the second annual report on a program to study the fundamentals of mesophase behavior that pertain to the processing of carbon-fiber-reinforced carbon-matrix composites. The work is supported by the Office of Naval Research (ONR) under Contract No. N00014-81-MP0006, work unit number NR 039-183. The principal investigator is J. L. White. The ONR scientific officer is L. H. Peebles, Jr.; his interest and support are gratefully acknowledged. We also thank M. Buechler, C. B. Ng, and F. B. Sinsheimer for their contributions to the experimental work; J. S. Evangelides and R. A. Meyer for technical consultation; and G. W. Smith (General Motors Research Laboratories) and J. E. Zimmer (Acurex Corporation) for technical collaboration.

|                    |                                     |
|--------------------|-------------------------------------|
| Accession For      |                                     |
| NTIS GRA&I         | <input checked="" type="checkbox"/> |
| DTIC TAB           | <input type="checkbox"/>            |
| Unannounced        | <input type="checkbox"/>            |
| Justification      |                                     |
| By _____           |                                     |
| Distribution/      |                                     |
| Availability Codes |                                     |
| Dist               | Avail and/or<br>Special             |
| A-1                |                                     |



## CONTENTS

|  |    |
|--|----|
| PREFACE.....   | 1  |
| I. INTRODUCTION.....                                     | 7  |
| II. MESOPHASE FORMATION WITHIN CARBON FIBER BUNDLES..... | 9  |
| A. Introduction.....                                     | 9  |
| B. Petroleum Pitch Impregnant.....                       | 11 |
| C. Coal-Tar Pitch Impregnant.....                        | 17 |
| D. Mesophase-Pitch Interfacial Energy.....               | 17 |
| E. Discussion.....                                       | 25 |
| III. MESOPHASE HARDENING.....                            | 27 |
| IV. PREPARATION OF MESOPHASE SPECIMENS.....              | 33 |
| V. FURTHER INVESTIGATIONS.....                           | 43 |
| VI. REPORTS, PUBLICATIONS, AND PRESENTATIONS.....        | 45 |
| REFERENCES.....  | 47 |

## FIGURES

|     |   |    |
|-----|---|----|
| 1.  | Fiber Bundle Holder.....  | 10 |
| 2.  | Mesophase Behavior in and around an Open Fiber Bundle.....  | 13 |
| 3.  | Mesophase Formation around Open Fiber Bundles.....  | 14 |
| 4.  | Mesophase Formation in High-Pressure Pyrolysis.....   | 15 |
| 5.  | Mesophase Formation in Room-Pressure Pyrolysis.....   | 16 |
| 6.  | Mesophase Formation in and around a Fiber Bundle<br>Impregnated with 15V Coal-Tar Pitch.....                | 18 |
| 7.  | Insoluble Aggregation in Bulk 15V Coal-Tar Pitch.....   | 19 |
| 8.  | Wetting Behavior within Fiber Bundles Impregnated with<br>15V Coal-Tar Pitch.....                           | 20 |
| 9.  | Wetting Behavior in T300 Fiber Bundles at Two Stages of<br>Mesophase Transformation.....                    | 21 |
| 10. | Wetting Behavior in P55 Fiber Bundles at Two Stages of<br>Mesophase Transformation.....                     | 22 |
| 11. | Coalescence of Mesophase Spherules.....   | 24 |
| 12. | Penetrometer Curves for Mesophase Pitches Prepared from<br>A240 Petroleum Pitch and 15V Coal-Tar Pitch..... | 29 |
| 13. | Softening Points of Mesophase Pitches as a Function of<br>Pyrolysis Temperature.....                        | 30 |
| 14. | Foamed Microstructures of Mesophase Pitch Prepared for<br>Extrusion and Draw Experiments.....               | 34 |
| 15. | Penetrometer Trace for Mesophase Pitch Used in Extrusion<br>and Draw Experiments.....                       | 35 |
| 16. | Schematic of Extrusion Device.....  | 36 |
| 17. | Microstructure of a Sound Mesophase Rod Extruded below 340°C.....   | 38 |
| 18. | Effect of Bubbles in Disrupting the Preferred Orientation of<br>Extruded Mesophase Rods.....                | 39 |

## FIGURES (Continued)

|  |    |
|--|----|
| 19. Effect of Drawing in Reorienting a Strongly Bubbled Mesophase Rod.....         | 40 |
| 20. Microstructure of a Sound Mesophase Rod Produced by Extrusion and Drawing..... | 41 |

## TABLE

|   |    |
|---|----|
| 1. Carbon Fibers Used in Pyrolysis Experiments..... | 11 |
|---|----|

## I. INTRODUCTION

Carbon-fiber-reinforced carbon-matrix composites have been established by their high-temperature properties as leading candidate materials for many structural applications demanding resistance to thermal shock, strength at temperature, and resistance to erosion by hot, high-velocity gas streams. Most fabrication processes for such composites form a pregraphitic matrix by impregnating a woven fiber preform with coal-tar or petroleum pitches that pass through a mesophase (liquid-crystal) state upon carbonization. Thus the carbonaceous mesophase plays a key role in fabrication because its behavior determines the microstructure of the composite matrix and the number of impregnation cycles required to reach desired levels of density.

That the mesophase transformation is essential in establishing the graphitizability of carbonaceous materials was first recognized by Brooks and Taylor in 1965.<sup>1,2</sup> This basic observation has since been pursued by carbon scientists interested in how the lamelliform morphology of graphitic materials forms during the carbonization of organic precursors. It is now well established that the principal microstructural features of coke and graphite originate during the brief plastic lifetime of the carbonaceous mesophase before it congeals to a solid semi-coke.<sup>3,4,5</sup>

This program's initial investigations<sup>6,7</sup> focused on identifying the patterns of mesophase formation within carbon fiber bundles. Several significant differences from mesophase formation in bulk pyrolysis were observed. The most striking observations, however, were the near-identical patterns of mesophase formation in the presence of various types of carbon fibers and the dominance of substrate-surface mesophase alignment in determining the matrix microstructures.<sup>8,9</sup>

In FY 83, mesophase formation within fiber bundles was explored further to understand the salient process variables for composite fabrication. Additional generalizations about microstructure-formation mechanisms in composite fabrication are emerging; for example, that wetting behavior is independent of pitch type,<sup>9</sup> and that the energy of the mesophase-pitch

interface is low.<sup>10</sup> The process of mesophase hardening was studied. Such hardening is significant to composite fabrication because it defines the thermal treatment beyond which high pressure should no longer be required to minimize mesophase movement caused by the percolation of pyrolysis gases. Work was also begun on preparing mesophase specimens with well-defined morphologies so that the effects of heat treatment on the microconstituents of carbon-matrix composites can be measured. Techniques of mesophase extrusion and draw show promise for the preparation of rods with fine fibrous micro-structure and strong preferred orientation.

## II. MESOPHASE FORMATION WITHIN CARBON FIBER BUNDLES

### A. INTRODUCTION

In previous studies of mesophase formation in petroleum-based precursors,<sup>11,12</sup> specimens of petroleum pitch quenched from various stages of pyrolysis were examined to learn how the mesophase morphologies of petroleum coke are formed. In this study, we applied the same technique of interrupted pyrolysis to pitch-impregnated fiber bundles that had been subjected to conditions common in composite processing. Because of the markedly different environmental conditions of composite processing--especially the proximity of the matrix pitch to fiber substrates and the elevated pressures used to improve the densification efficiency--the patterns of mesophase formation in the fiber bundles were expected to be markedly different from those in petroleum coke. The mesophase's fluid state may extend over a wider temperature range than in room-pressure pyrolysis, and surface forces and alignment effects may be the major factors in determining the matrix morphology within a fiber bundle.<sup>8,13</sup>

The experimental techniques have been detailed in previous reports.<sup>6,7,14</sup> Figure 1 shows the fixture used to hold the fiber bundles within a tubular pyrolysis cell and to define the micrographic sections. All micrographs of fiber bundles in this report are transverse sections of the open bundle (section C), which approximates a fiber bundle adjacent to a weave cavity in a three-dimensional (3D) reinforced composite. The room-pressure specimens were prepared by heating a set of pyrolysis cells within a large copper block to ensure equivalent and smooth heating. Specimens were removed at temperatures of interest and quenched by insertion into a cold copper block. The high-pressure specimens were prepared individually by heating within a furnace of low thermal inertia operating inside a cold-wall autoclave; at high pressure the thermal coupling is sufficient to obtain effective quenching by switching off the power to the small furnace.

Work reported previously<sup>6-9</sup> dealt primarily with an insoluble-free petroleum-pitch impregnant (Ashland A240) pyrolyzed at room pressure. The

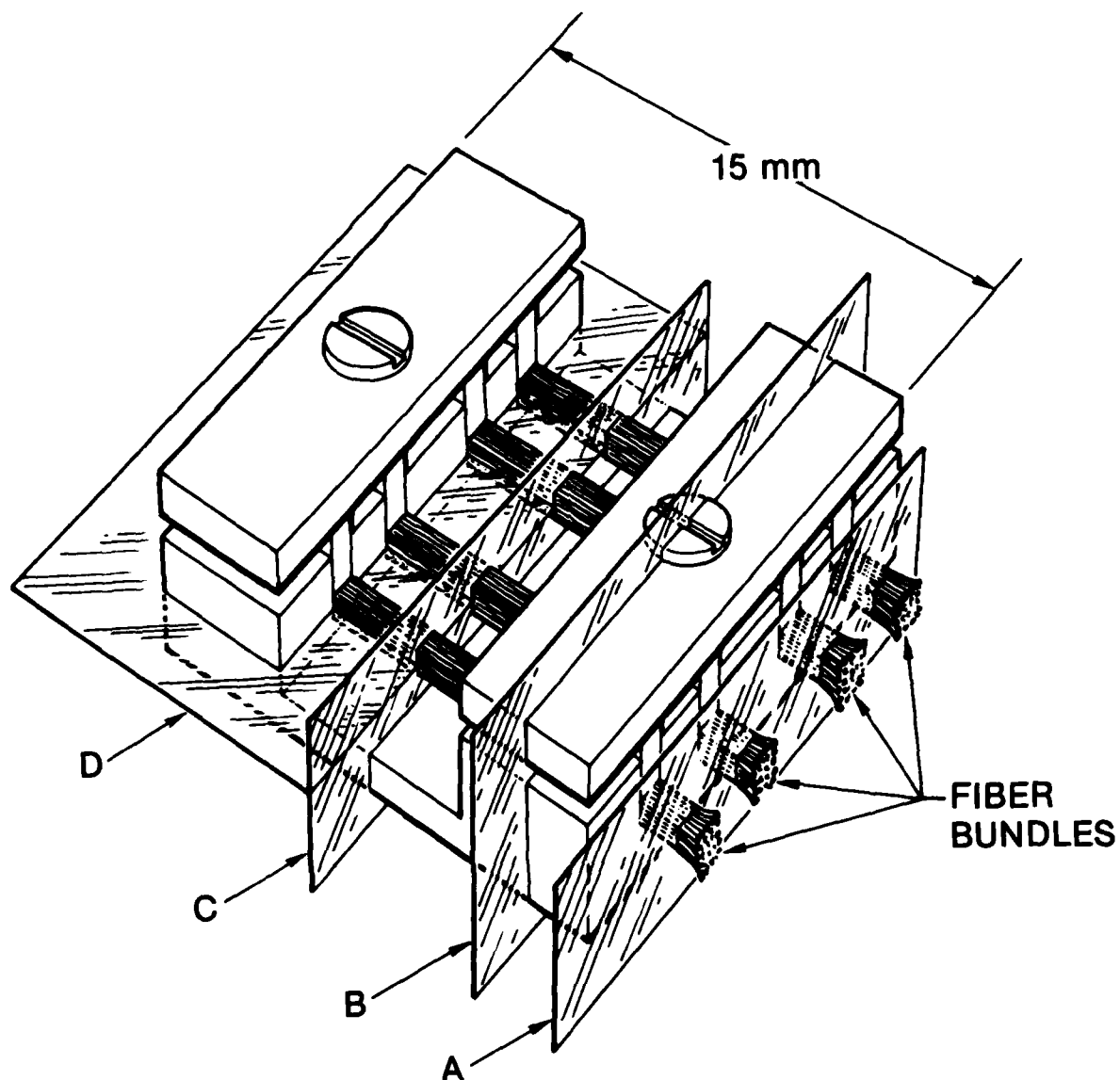


Fig. 1. Fiber Bundle Holder. The aluminum fixture holds four fiber bundles during pyrolysis in a pool of impregnant pitch. Planes A, B, and C define transverse sections for splayed, constrained, and open bundles, respectively; and plane D defines a longitudinal section for the four fiber bundles. Reproduced from Ref. 6.

mesophase transformation was observed to proceed more slowly within a fiber bundle, without the extensive deformation characteristic of mesophase pyrolyzed in bulk. All fibers studied, including PAN-based and mesophase-based fibers, were wetted by both pitch and mesophase. The porosity developed within a bundle was coarser for less constrained bundles. When the mesophase hardened, it behaved as a fragile solid easily fractured by local stresses within the fiber bundle. The work reported here extends these observations and shows that the pyrolysis behavior of a coal-tar-pitch impregnant (Allied 15V) is similar in most respects to that of the petroleum pitch. The four fibers studied are listed in Table 1.

Table 1. Carbon Fibers Used in Pyrolysis Experiments

| Designation <sup>a</sup> | Type      | Shape      | Diameter <sup>b</sup><br>( $\mu\text{m}$ ) | Nominal Tensile Modulus<br>(Mpsi) | Modulus<br>(GPa) |
|--------------------------|-----------|------------|--|-----------------------------------|------------------|
| T300                     | PAN-based | Near-round | 7.0  | 35                                | 240              |
| VSA-11                   | Mesophase | Open Wedge | 14.8                                       | 50                                | 345              |
|                          |           | Round      | 14.0                                       |                                   |                  |
| P55                      | Mesophase | Round      | 10.7                                       | 55                                | 380              |
| P100                     | Mesophase | Oval       | 10.2                                       | 100                               | 690              |

<sup>a</sup>Source for all fibers: Union Carbide Corporation.

<sup>b</sup>Diameter, or largest transverse dimension, for typical filaments.

#### B. PETROLEUM PITCH IMPREGNANT

The behavior of A240 petroleum pitch is typical of most binder and impregnant pitches: It exhibits strong bloating when pyrolysis reaches the point at which the mesophase becomes the continuous phase.<sup>14,15</sup> If bloating occurs in a pitch-impregnated composite, it may constitute a "blow-out" mechanism that could account for the low coke yields observed in composite processing.<sup>16</sup> We sought evidence of bloating and mesophase movement within fiber bundles by examining a series of pitch-impregnated specimens pyrolyzed into and through the mesophase transformation, but observed no strong

effects--no deformed mesophase or sudden increases in porosity within bundles when the mesophase transformation neared completion. Figure 2 demonstrates that strong bloating occurred outside a fiber bundle, producing large bubbles and highly deformed bubble walls; however, within the bundle the mesophase microstructure evidences no deformation effects and the porosity appears only marginally greater than before transformation was completed. Such behavior was common to all fibers studied, as was the alignment of the mesophase layers parallel to the fiber substrate.

We next attempted to check whether these observations could be extended to high-pressure pyrolysis, but were limited by frequent failures of the heating element operating within the cold-wall autoclave. The furnace was originally designed with minimal electrical insulation to attain low thermal inertia and rapid cooling rates, but this insulation proved inadequate to avoid shorting and burnout when the furnace atmosphere became laden with hydrocarbons from the pyrolyzed specimen. This problem has since been corrected by using a fully sheathed heater, with only slightly greater thermal inertia.

Figure 3 compares mesophase formation in A240 petroleum pitch pyrolyzed to 450°C under 5000 psi with a specimen pyrolyzed to 438°C at room pressure. In both specimens, pyrolysis had reached the condition of rapid mesophase transformation outside the fiber bundles, and mesophase layers tended to form around the open fiber bundles. However, the specimen pyrolyzed at high pressure displays inhibited coalescence and coarser microstructures, apparently caused by the lesser degree of stirring and deformation by bubble percolation.

As illustrated by Fig. 4 for the specimen pyrolyzed under 5000 psi, the mesophase transformation within the fiber bundles has only just begun at 450°C. The wetting behavior with the pitch-mesophase interface standing near normal to the substrate is similar to that observed in room-pressure pyrolysis; Fig. 5 illustrates approximately the same level of transformation in pyrolysis under room pressure at 5°C/hr to 429°C.

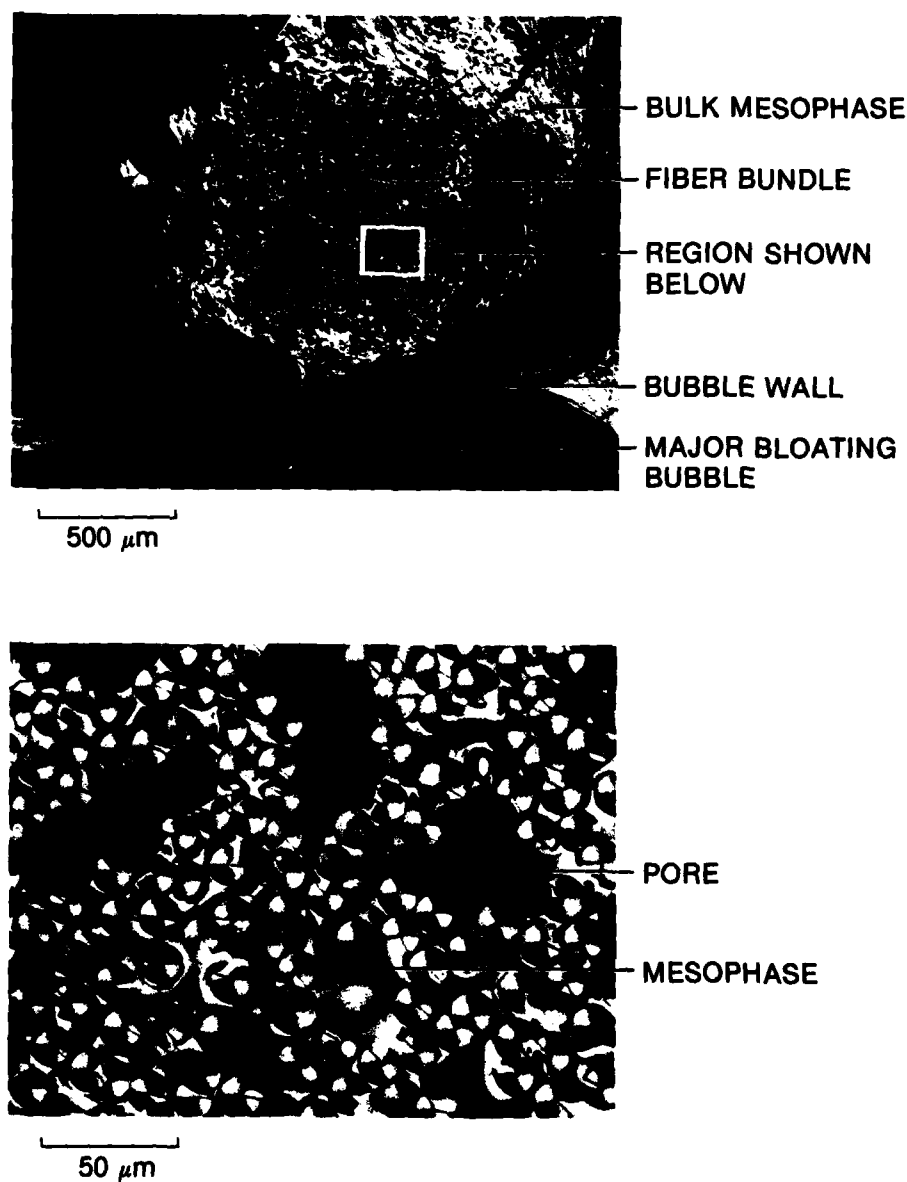
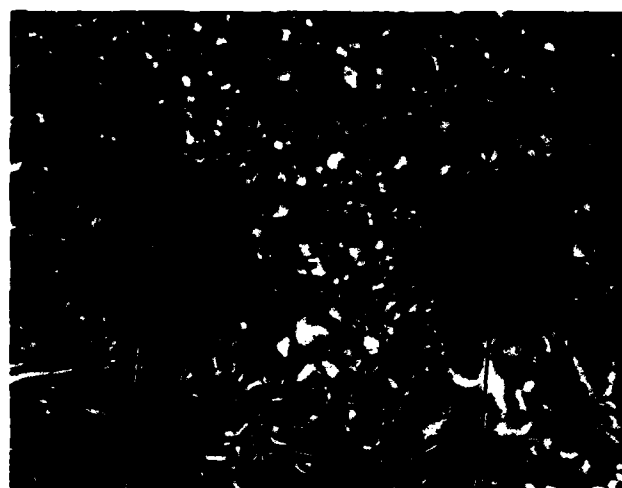


Fig. 2. Mesophase Behavior in and around an Open Fiber Bundle. Room-pressure pyrolysis of VSA-11 mesophase-based fiber in A240 petroleum pitch at 5°C/hr to 464°C. Partially crossed polarizers.



**HIGH PRESSURE**  
5000 psi, 450°C

VSA-11  
BUNDLE

T300  
BUNDLE

P55  
BUNDLE

P100  
BUNDLE



**ROOM PRESSURE**  
438°C

PORE

1 mm

**Fig. 3. Mesophase Formation around Open Fiber Bundles.** Room pressure pyrolysis at 5°C/hr; 5000-psi pyrolysis heated at 10°C/hr. Partially crossed polarizers.

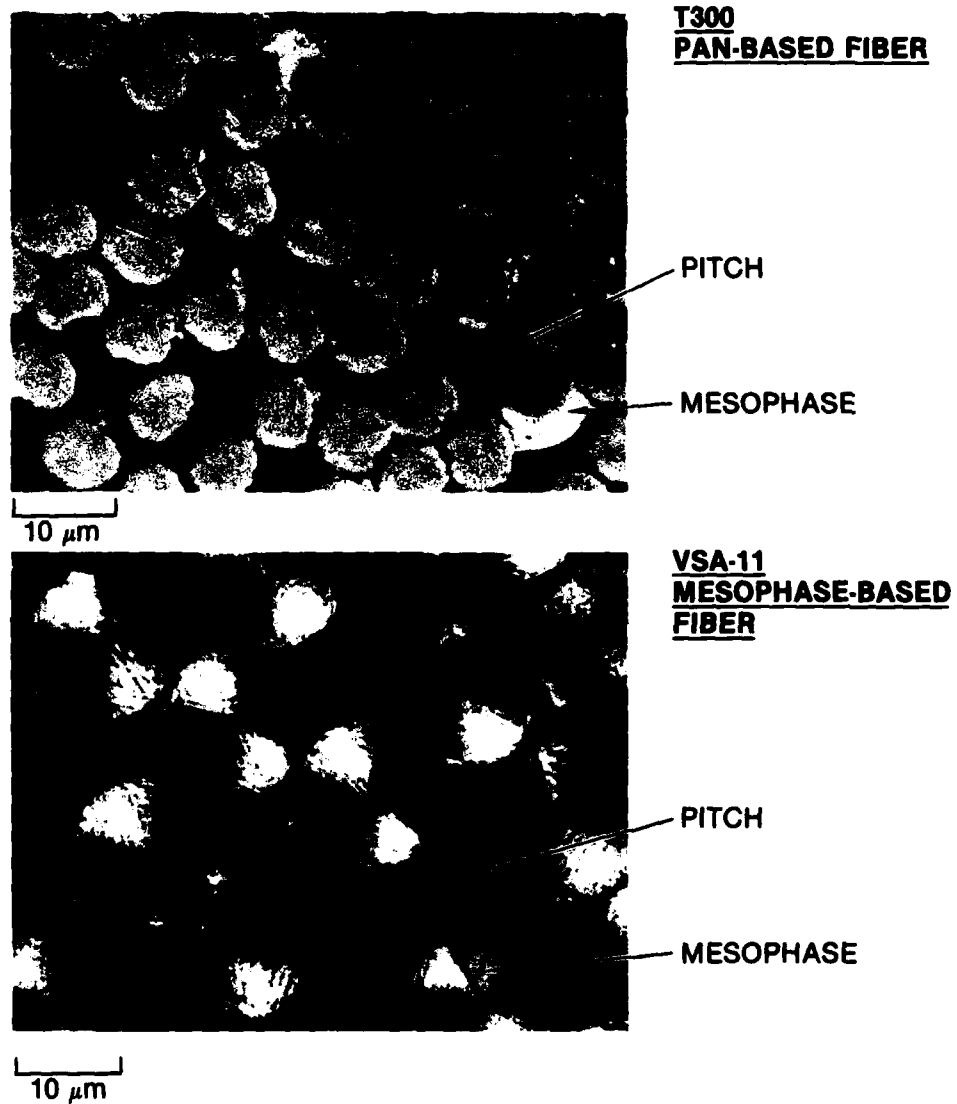


Fig. 4. Mesophase Formation in High-Pressure Pyrolysis. Pyrolysis of A240 petroleum pitch under 5000 psi in open fiber bundles at 10°C/hr to 450°C. Partially crossed polarizers.

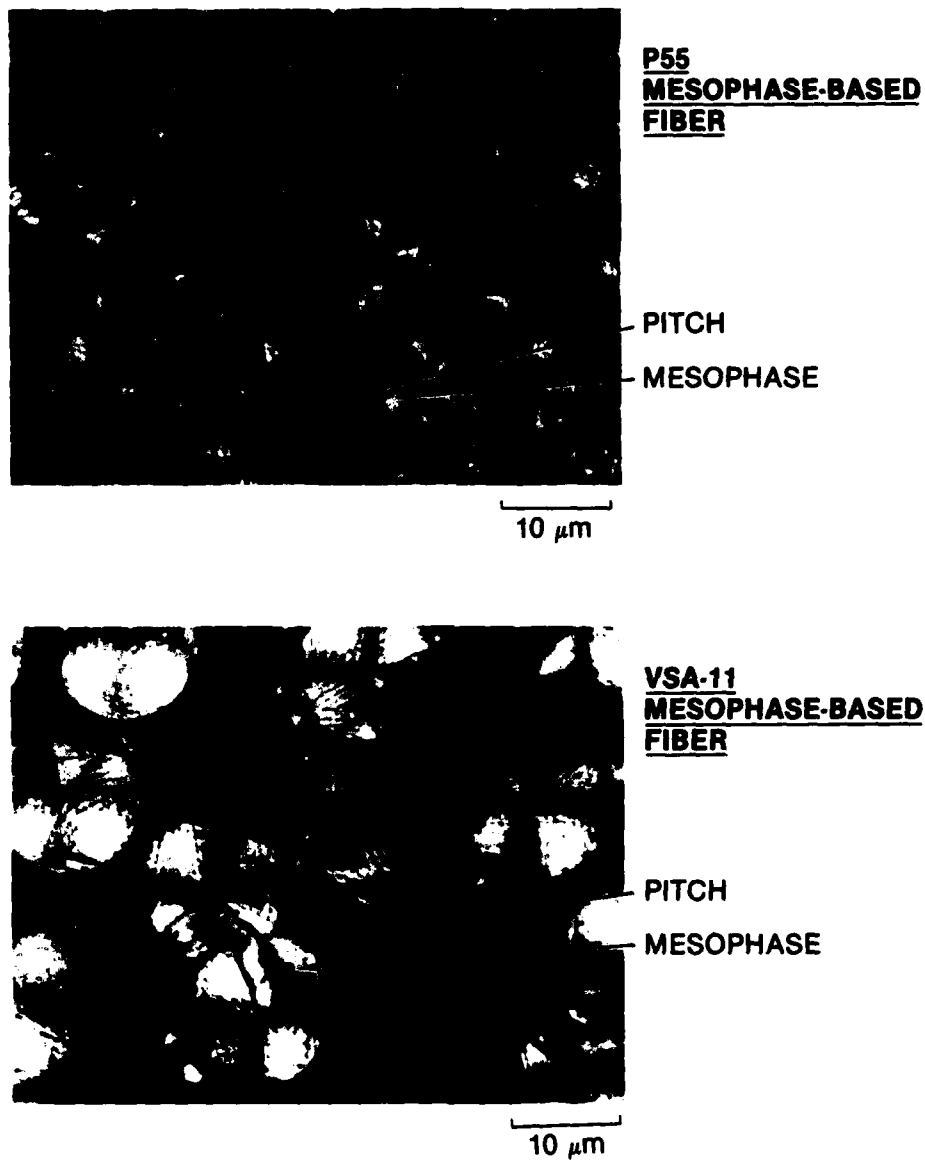


Fig. 5. Mesophase Formation in Room-Pressure Pyrolysis. Room-pressure pyrolysis of A240 petroleum pitch in open fiber bundles at 5°C/hr to 429°C. Partially crossed polarizers.

### C. COAL-TAR PITCH IMPREGNANT

Mesophase formation within fiber bundles impregnated with a coal-tar pitch (Allied 15V) has been studied further. The previous annual report<sup>7</sup> illustrated how the fiber bundle acts as a filter to remove a fraction of the insoluble particles from the pitch that enters the bundle. This effect at an early stage of pyrolysis is depicted by Fig. 6, the higher-magnification view within the bundle demonstrating that the insoluble particles that penetrate into the bundle tend to aggregate in much the same manner as in bulk pitch. Figure 7 illustrates the aggregation mechanisms in the bulk pitch. Segregation first occurs to form insoluble-rich regions, then a sweeping action takes place as the mesophase transformation proceeds in the insoluble-poor regions to collect the particles at the mesophase-pitch interface.<sup>3</sup>

The wetting behavior within fiber bundles impregnated with 15V coal-tar pitch is illustrated by Fig. 8 for a pyrolysis condition in which both mesophase and pitch are present. Although the insoluble particles make both micrographic preparation and observation more difficult, the wetting behavior appears to be the same as observed for A240 petroleum pitch: The pitch wets the filaments with near-zero wetting angle, and the pitch-mesophase interface stands near-normal to the filament surface. Agglomeration by both insoluble segregation and interface collection appears to operate on the scale of inter-filament distances.

Wetting conditions after the mesophase transformation is complete are compared with those early in the transformation for two types of fiber (PAN-based T300 and mesophase-based P55) in Figs. 9 and 10. Similar views were obtained for VSA-11 and P100 fibers. The mesophase-pore surfaces in the fully transformed samples show that the mesophase wets the filaments at a near-zero angle. In general, the filaments are more densely packed after transformation is complete, except in regions of heavy insoluble agglomeration.

### D. MESOPHASE-PITCH INTERFACIAL ENERGY

Four points indicate that the surface energy of a mesophase-pitch interface in a partially transformed pitch is low:

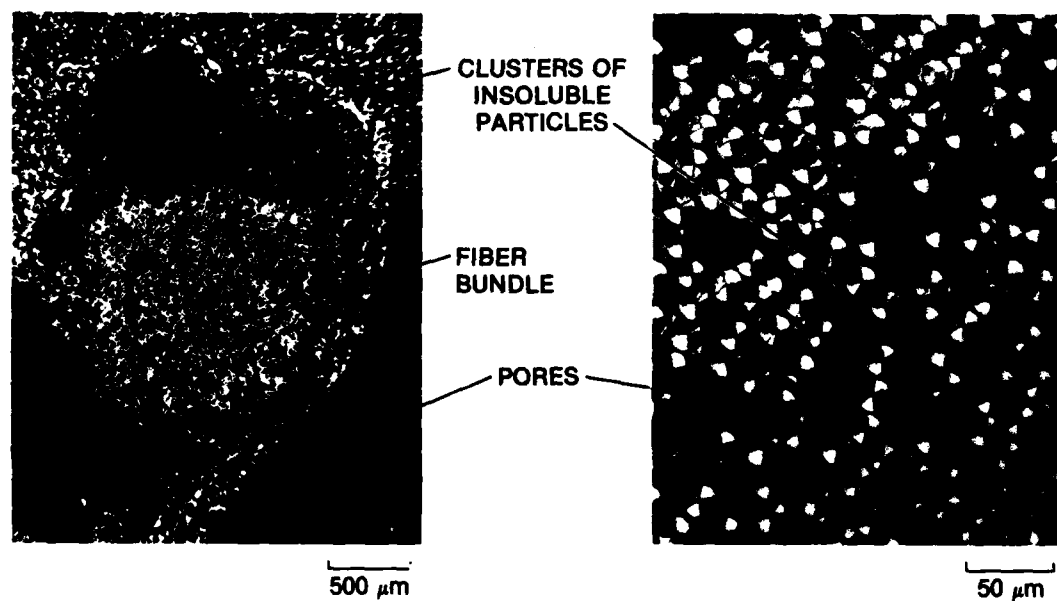
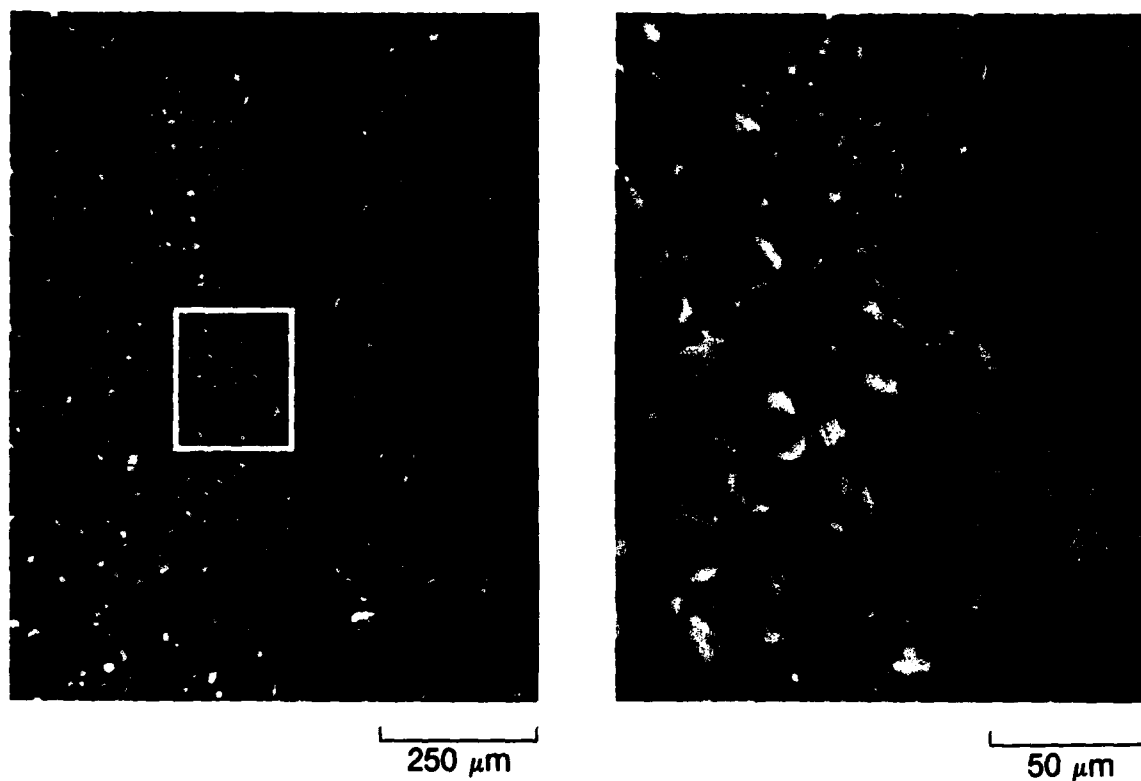


Fig. 6. Mesophase Formation in and around a Fiber Bundle Impregnated with 15V Coal-Tar Pitch. Magnified view of central portion of fiber bundle in left-hand micrograph is given in right-hand micrograph. Room-pressure pyrolysis at 5°C/hr to 438°C; VSA-11 fiber. Partially crossed polarizers.



**Fig. 7.** Insoluble Aggregation in Bulk 15V Coal-Tar Pitch. Room-pressure pyrolysis at 5°C/hr to 429°C; partially crossed polarizers. Boxed region in left micrograph is enlarged in right micrograph.

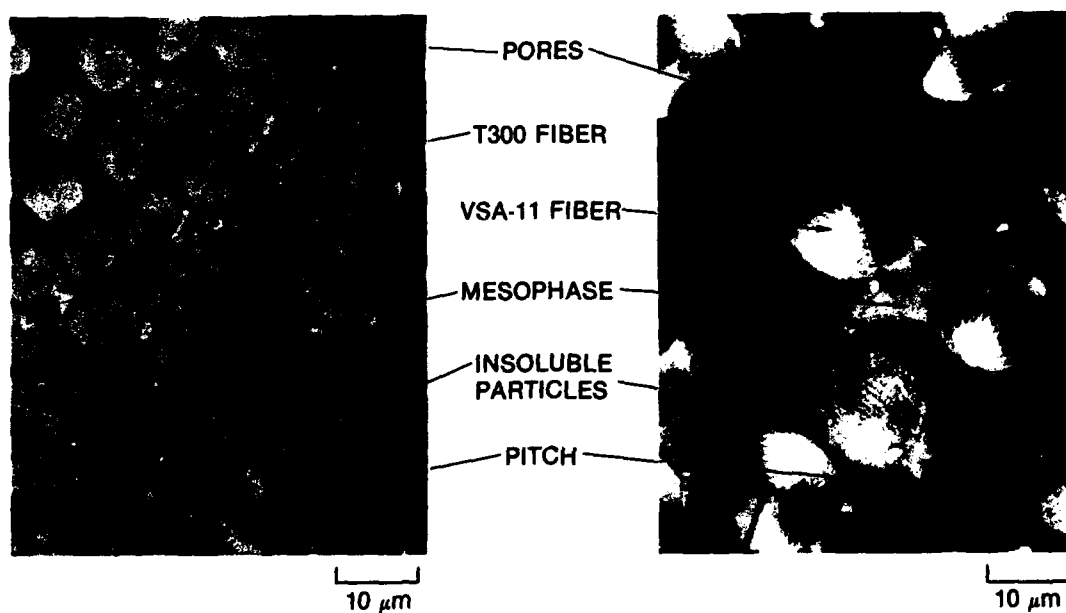


Fig. 8. Wetting Behavior within Fiber Bundles Impregnated with 15V Coal-Tar Pitch. Room-pressure pyrolysis at 5°C/hr to 438°C; partially crossed polarizers, oil immersion.

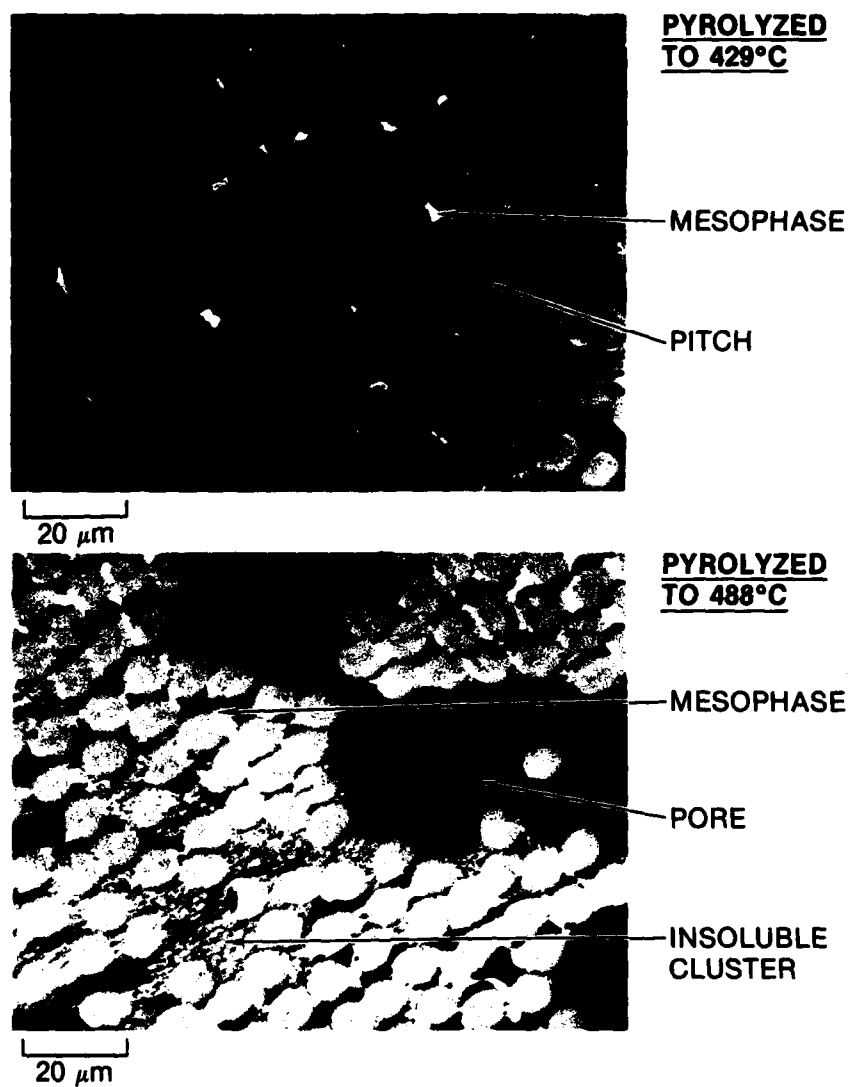


Fig. 9. Wetting Behavior in T300 Fiber Bundles at Two Stages of Mesophase Transformation. Room-pressure pyrolysis at 5°C/hr; partially crossed polarizers.

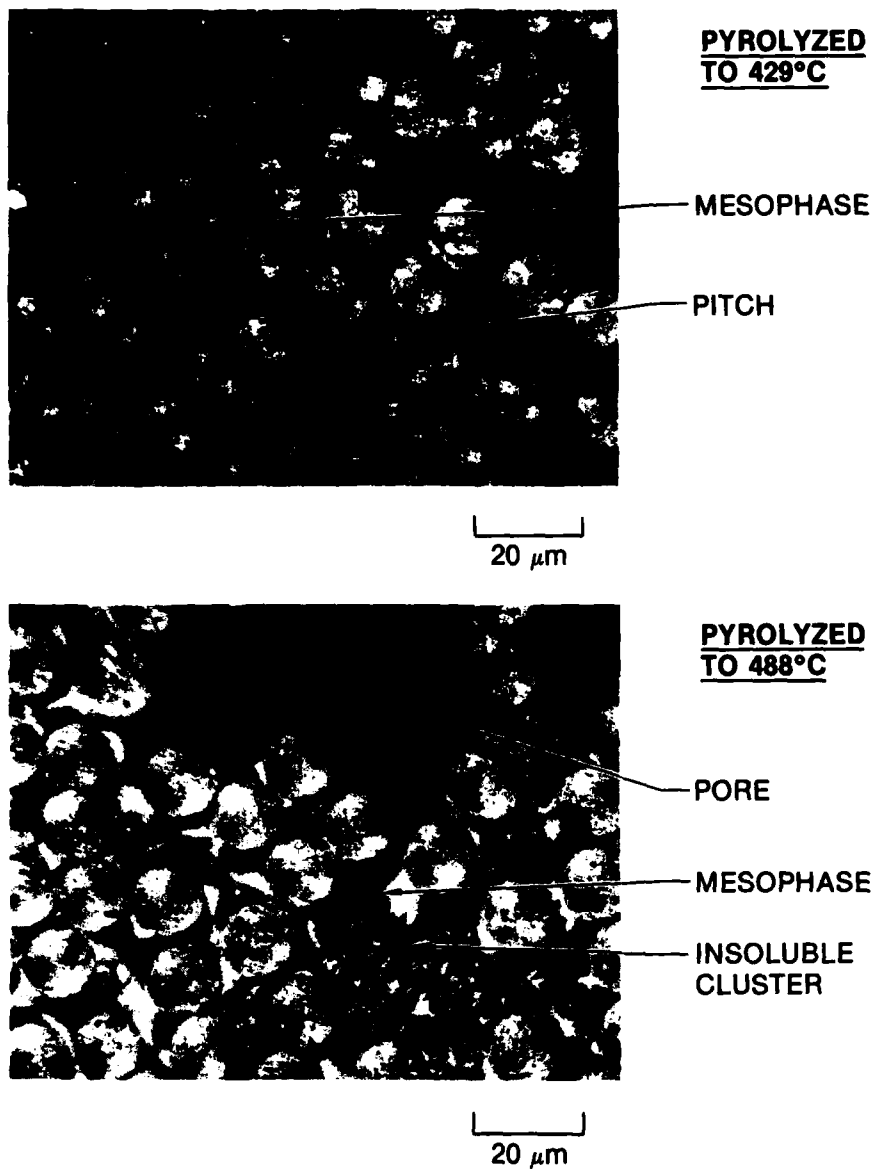


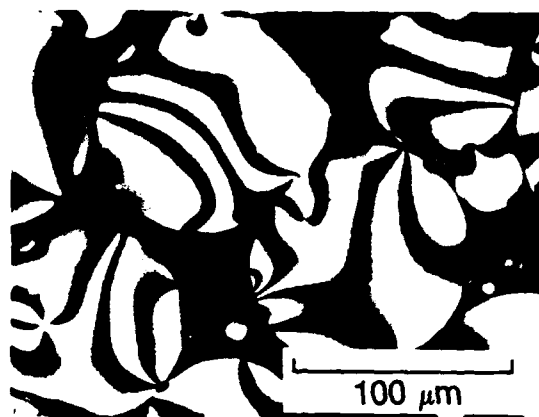
Fig. 10. Wetting Behavior in P55 Fiber Bundles at Two Stages of Mesophase Transformation. Room-pressure pyrolysis at 5°C/hr; partially crossed polarizers.

1. The conclusion by Cranmer et al.<sup>13</sup> based on their observations that the mesophase forms by homogeneous nucleation independent of the type of carbon surface in the vicinity of the pyrolyzing pitch.
2. The present observations of little or no preference to wetting by mesophase or pitch, as in the near-normal orientation of the mesophase-pitch interface relative to the filament surface, demonstrating that wetting energies are nearly the same for both phases.
3. The fact that filament packing seems to proceed further in the presence of mesophase-pore surfaces than in the presence of mesophase-pitch interfaces.
4. Observations by the quenching hot-stage microscope<sup>17</sup> that the free surface near intersection with a mesophase-pitch interface is flat and undistorted, consistent with a low value for the interfacial energy.

When these points were discussed at the Sixteenth Conference on Carbon,<sup>9</sup> G. W. Smith of the General Motors Research Laboratory pointed out that an independent estimate of the mesophase-pitch interfacial energy could be made by applying Frenkel's relation<sup>18</sup> for fusion by viscous flow to hot-stage observations of mesophase coalescence:

$$\tau = \frac{\eta R}{\sigma} \quad (1)$$

where  $\tau$  is the time constant for coalescence,  $\eta$  is the viscosity,  $\sigma$  is the interfacial energy, and  $R$  is the radius of two coalescing spherules assumed to be of equal size. A frame-by-frame analysis of films of three coalescence events, such as those in Fig. 11, led Smith to estimate values of 0.003 to 0.2 dyne/cm for the mesophase-pitch interfacial energy, which are markedly smaller than values of 20 to 50 dyne/cm for the surface energies of typical organic liquids. The principal uncertainty in the calculation lies in the viscosity value. In any case, the interfacial energy is very low compared with typical surface energies, and the deductions from the micrographic observations are confirmed. These results have been prepared for publication.<sup>10</sup>



(a)



(b)



(c)

Fig. 11. Coalescence of Mesophase Spherules: (a) initial spherule contact; (b) partial coalescence to produce a "waist"; (c) disappearance of the waist. Observed on free surface by hot-stage microscopy on A240 petroleum pitch at 440°C; crossed polarizers. From Ref. 10.

## E. DISCUSSION

The wetting behavior by both pitch and mesophase is independent of fiber type, at least for the four fibers studied to date. This common behavior also extends to the pattern of mesophase formation during pyrolysis and to the alignment of the mesophase layers parallel to the fiber surface; and it applies to coal-tar pitch as well as petroleum pitch, providing that allowance is made for the perturbing influence of the insoluble particles in the coal-tar pitch. Such commonality in behavior also seems to hold, at least for the petroleum pitch, for pyrolysis to pressure levels of 5000 psi, and thus promises to reduce appreciably the experimentation required to characterize mesophase formation under practical processing conditions.

Although the filaments in the outer rim of a fiber bundle appear to filter a portion of the insoluble particles from coal-tar pitch, a substantial fraction of the insolubles reaches the interior of the fiber bundle even for the finest fiber (T300) studied. Upon pyrolysis, the mechanisms of insoluble agglomeration act in much the same way as in bulk pitch, leaving an obviously microheterogeneous matrix within the fiber bundle. These microheterogeneities thus set the stage for the development of distortions and local stresses when the composite is heat-treated.

Strong bloating effects within fiber bundles have not been observed, even when the bulk mesophase outside the bundle shows the effects of strong deformation by bubble percolation. This qualitative micrographic evidence does not permit the conclusion that bloating effects do not occur, but only that bloating does not cause sudden increases in bundle porosity and that the tendency for mesophase to align with fiber surfaces is strong enough to reorient any deformed morphologies that might have been produced by mesophase movement. In fact, the tendency to mesophase alignment operating over the short interfila-ment distances within a fiber bundle totally dominates the formation of matrix microstructure, and the disclination structures within the bundle appear to be predictable from the geometry of filaments surrounding each matrix channel.<sup>8,19</sup>

The determination from coalescence kinetics that the mesophase-pitch interfacial energy is low relative to mesophase or pitch surface energies confirms inferences from several micrographic observations. The practical implication for composite processing is that porosity agglomeration, observed when filaments are not tightly constrained in the fiber bundle,<sup>6</sup> must be due to pitch or mesophase surface tensions acting in regions that are already porous because of gas evolution during pyrolysis.

### III. MESOPHASE HARDENING

The purpose of high-pressure processing in composite fabrication is to attain higher densities in each impregnation cycle, presumably by retaining as much matrix pitch as possible within the 3D preform until the mesophase has formed and hardened. Thus, economically, it is desirable to know the pyrolysis intensity required to fix the matrix in place--the point in thermal treatment beyond which high-pressure processing is required no further. The mechanism of mesophase hardening defines this point and the point at which the lamelliform morphology of the carbonaceous mesophase is locked into place.

Although mesophase hardening has practical and basic significance, we are unaware of systematic studies of it. However, investigations<sup>20-22</sup> of the viscosity of pyrolyzing pitch indicate some aspects of the behavior to be expected. When the pyrolysis temperature reaches levels at which volatilization and aromatic polymerization become rapid, the viscosity rises sharply and rapidly surpasses the range of typical viscometers. Balduhn and Fitzer<sup>22</sup> found that this critical temperature level depends strongly on the nature of the pitch and even on the shear rate during pyrolysis in the viscometer; e.g., for a set of five pitches of varied origins, the temperature at which the viscosity reached 100 poise ranged from 430 to 520°C. At high pressure, the volatile compounds tend to be retained in the pyrolyzing mass, and the hardening point may be appreciably higher than observed at room pressure.

In the present work, we are examining a temperature-programmed penetrometer test as a means of determining whether a mesophase specimen has been sufficiently pyrolyzed to undergo no softening in subsequent thermal treatment. The apparatus is a DuPont Thermomechanical Analyzer (Model 943) with a 2.5-mm-diam probe that can carry a load up to 100 g; the tests described here were made with 10-g loading, which corresponds to a pressure of 2.6 psi at the tip of the penetrometer probe. The powdered sample is contained in a 6-mm-diam silica cell, into which it is shaken and tamped to attain a depth of 5 mm. The penetrometer cell is heated at the rate of 5°C/mm, and the sample is protected against oxidation by a stream of nitrogen flowing through the heated cavity.

A series of mesophase specimens was prepared from A240 petroleum pitch and 15V coal-tar pitch under standardized pyrolysis conditions at room pressure to test the suitability of the penetrometer for defining the pyrolysis condition for effective hardening. The samples were pyrolyzed at 5°C/hr to finishing temperatures that ranged from 441 to 507°C. The pyrolysis yields were reproducible to better than ±1% and followed patterns previously reported.<sup>12</sup> After pyrolysis, the residues were crushed and sieved to -140/+325 mesh (44 to 105 µm particle size).

Figure 12 presents traces of five penetrometer tests, with the probe penetration plotted as a function of cell temperature. If the specimen softens appreciably, the probe penetrates to the bottom of the cell, and some well-defined point on the penetration curve can be taken arbitrarily as the softening point. If the specimen has been pyrolyzed to the point of effective hardening, the penetrometer trace shows only a gentle maximum near 450°C, where coke shrinkage overtakes the normal thermal expansion. Borderline cases of partial penetration occur when the pyrolysis condition approaches effective hardening. If a viscous specimen bloats by gases generated during the penetrometer run, a "lift-back" phenomenon is sometimes observed.

Figure 13 summarizes the results of a number of penetrometer runs on the two types of mesophase pitch. The softening point (for 1-mm penetration with 10-g loading) is plotted as a function of the pyrolysis temperature. For both materials, the specimens pyrolyzed to 466°C showed measurable softening points at 1-mm penetration (with one exception), whereas those pyrolyzed to the next temperature level at 476°C did not yield to the penetrometer load. The pyrolysis conditions for hardening thus lie between 466 and 476°C. The plot of softening points indicates further that the 15V-based mesophase hardens about 9°C higher than the A240-based mesophase, assuming that the viscosity curves on pyrolysis follow similar patterns. Note also that the softening point near the hardening condition is very sensitive to the pyrolysis temperature, i.e.,

$$\frac{dT_{\text{pen}}}{dT_{\text{pyr}}} \sim 9 \quad (2)$$

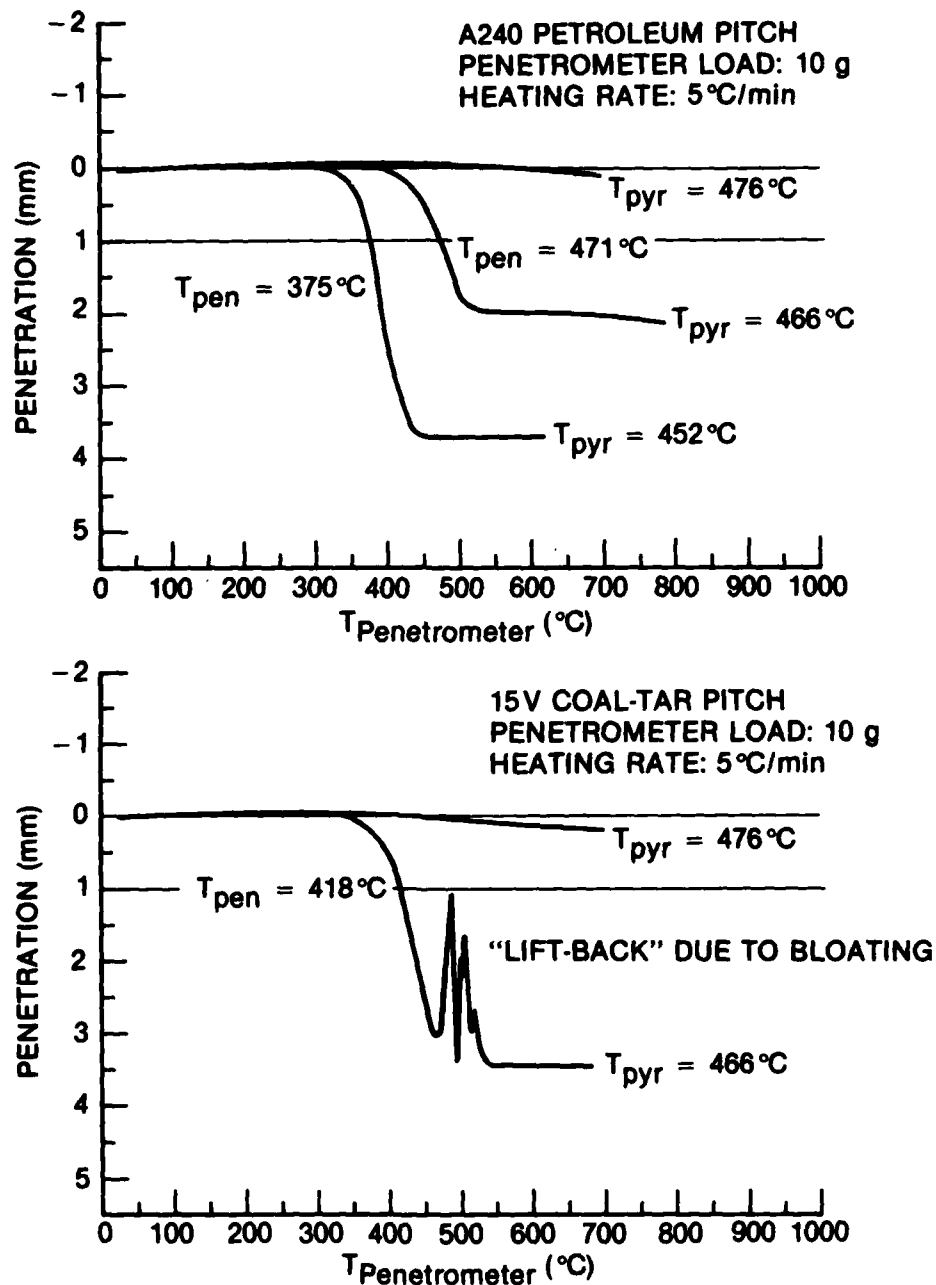


Fig. 12. Penetrometer Curves for Mesophase Pitches Prepared from A240 Petroleum Pitch and 15V Coal-Tar Pitch. Pyrolysis condition is given by  $T_{\text{pyr}}$ , the maximum temperature attained in standard pyrolysis at 5°C/hr. Softening point  $T_{\text{pen}}$  is penetrometer temperature corresponding to 1-mm penetration in a bed 5 mm deep.

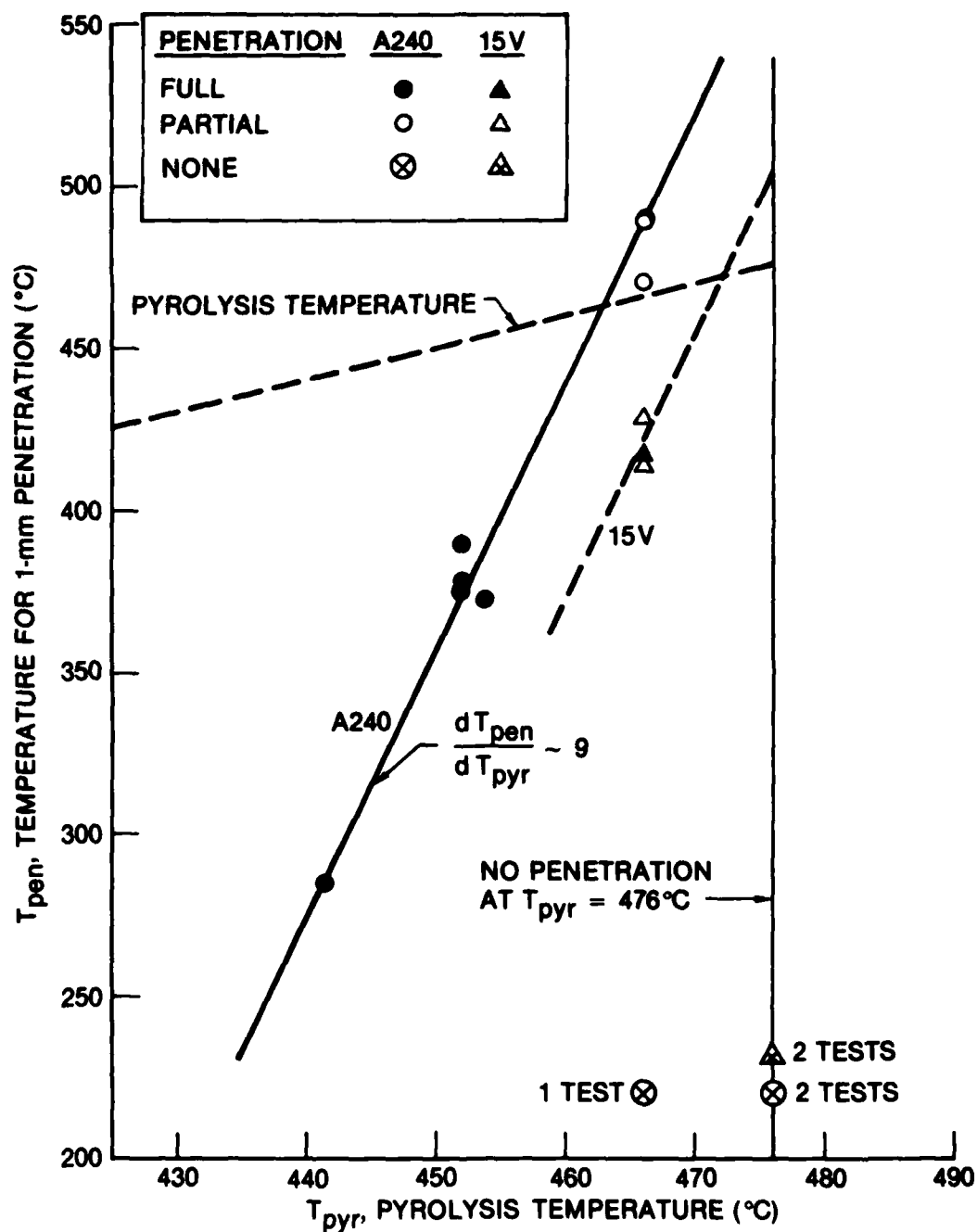


Fig. 13. Softening Points of Mesophase Pitches as a Function of Pyrolysis Temperature

where  $T_{\text{pyr}}$  is the temperature to which the specimen was pyrolyzed and  $T_{\text{pen}}$  is the softening point determined by the penetrometer.

The penetrometric method has thus been demonstrated to offer a means of defining mesophase hardening. Tests on pitches pyrolyzed under high pressure will be run to determine whether bloating effects from the release of dissolved gases disturb the measurement.

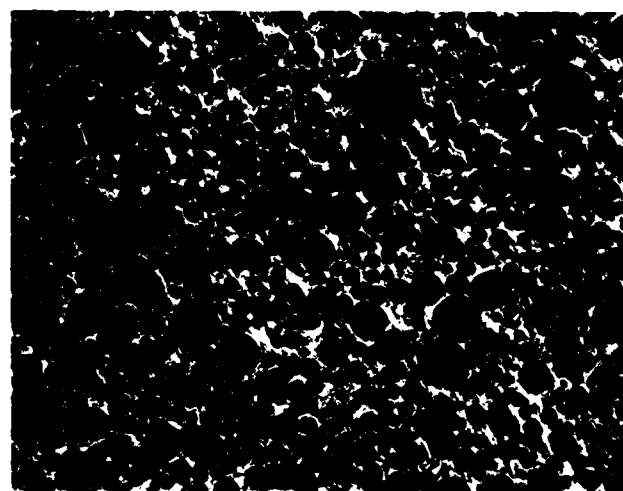
#### IV. PREPARATION OF MESOPHASE SPECIMENS

One objective of the present program is to obtain basic data on mesophase shrinkage, thermal expansion, and mechanical properties as a function of heat treatment, commencing from the point of mesophase hardening. Mesophase specimens of well-defined morphology in the just-hardened state are required. The experimental approach in the work described here was to explore extrusion and draw methods<sup>12,23</sup> to produce mesophase rods with fibrous microstructure.

The mesophase pitch was prepared from A240 petroleum pitch by the Chwastiak procedure,<sup>24</sup> i.e., stirred extensively and sparged with nitrogen; the heating schedule was 25°C/hr to 400°C and a 20-hr hold at 400°C. The yield was 44 wt% (including transfer losses). The microstructure depicted in Fig. 14 reveals full transformation to mesophase and consists of a thick-walled foam with the bubbles generally less than 1-mm in diameter. The spherical bubbles and the coarse texture of polarized-light extinction contours indicate that the mesophase was fluid at the preparation temperature. The pitch was crushed and compacted to 4000 psi at 200°C to minimize the porosity of the material to be melted down in the extrusion device.

The penetrometer trace of Fig. 15 shows a softening point of 309°C and the apparent commencement of bloating at about 340°C, well below the preparation temperature of 400°C. The tendency to bubble formation recommends the use of extrusion temperatures below 340°C to obtain sound, bubble-free extrudates.

The extrusion device diagrammed in Fig. 16 is similar to devices used to spin monofilaments of mesophase fiber.<sup>25</sup> The extrusion chamber and the spinnerette are constructed of aluminum for good thermal uniformity. The cell can be pressurized with nitrogen up to 300 psi. Three sizes of spinnerette orifices were used: 0.2, 0.9, and 2 mm in diameter. The figure shows how a weight can be clamped to the extruded rod to add draw to the extrusion process. The extent of draw is determined by the nitrogen-flow cooling action, as well as by the size of the attached weight.



2 mm



0.5 mm

Fig. 14. Foamed Microstructure of Mesophase Pitch Prepared for Extrusion and Draw Experiments

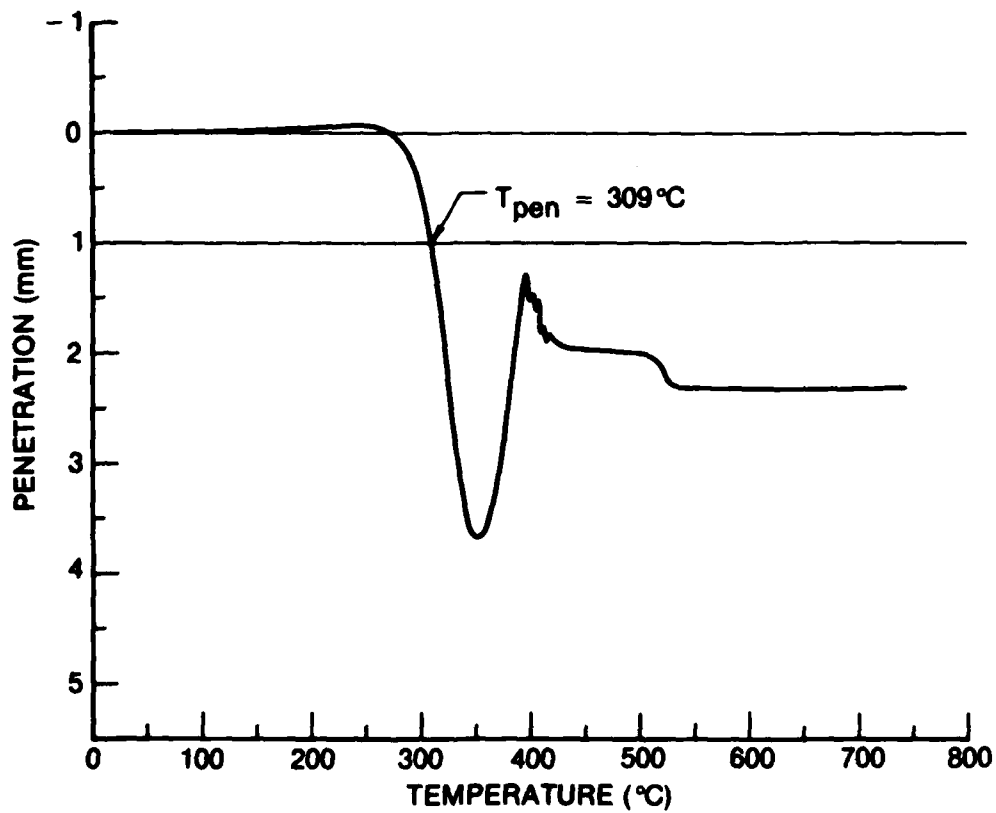


Fig. 15. Penetrometer Trace for Mesophase Pitch Used in Extrusion and Draw Experiments

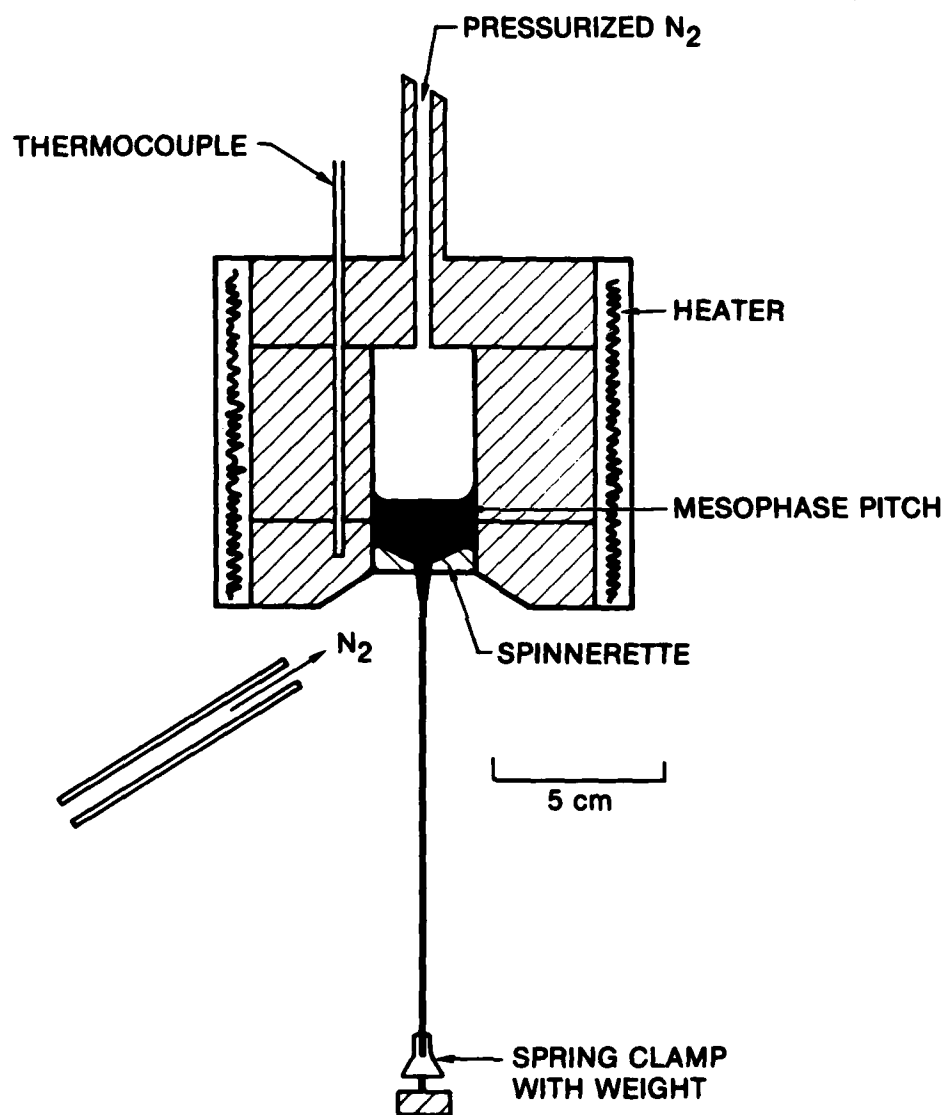


Fig. 16. Schematic of Extrusion Device. A weight can be attached to extruded rod to obtain draw following extrusion.

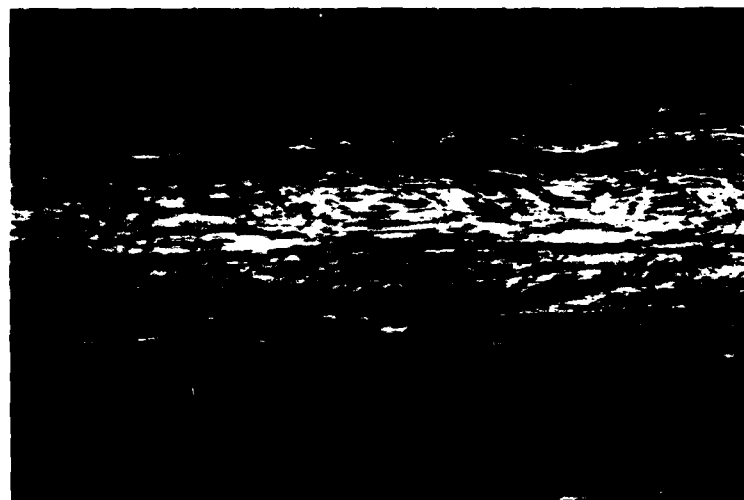
Extrusion was explored at temperatures of 320 to 410°C. Extrusion rates were very slow at the lower temperatures, e.g., 250 psi was required to attain a rate of 1 cm/min at 325°C with the 0.9-mm-diam orifice. The extrusion rate increased rapidly with temperature, but bubbles in the extrudate began to be visible at 340°C and were abundant above 375°C.

Figure 17 illustrates the microstructure of a sound extrusion obtained below 340°C with the 0.9-mm orifice. The longitudinal section shows relatively smooth flow, although some traces of the parabolic flow contours are visible because of small ripples in the flow. The transverse section reveals a fine fibrous microstructure with some tendencies to laminar preferred orientations in the rim. The diameter of 1000  $\mu\text{m}$  shows appreciable die swell when extrusion is employed without draw, behavior observed by Nazem.<sup>26</sup>

Bubbles appeared in the extrudate at temperatures above 340°C and at lower temperatures for long dwell times. As Fig. 18 illustrates, the presence of bubbles disturbs the preferred orientation; as the bubble frequency increases, the flow pattern is increasingly disrupted, eventually effecting a foamed rod with near-random microstructure.

Simple hand-drawing from the 2-mm orifice confirmed that drawing is effective in orienting even a heavily bubbled rod (see Fig. 19), and led to the more controlled drawing experiments with the weight attached to the extruded rod as depicted in Fig. 16. In one experiment, stable drawing conditions were found at 330°C and 140-psi extrusion pressure with the 0.9-mm orifice. As illustrated by Fig. 20, a rod of near-uniform diameter and fine fibrous microstructure was drawn at about 4 cm/min. The diameter was about 640  $\mu\text{m}$ , and the draw weight corresponded to a maximum stress of 24 psi. The draw rate and diameter were somewhat influenced by the cooling effect of the nitrogen stream directed to minimize oxidation near the extrusion orifice.

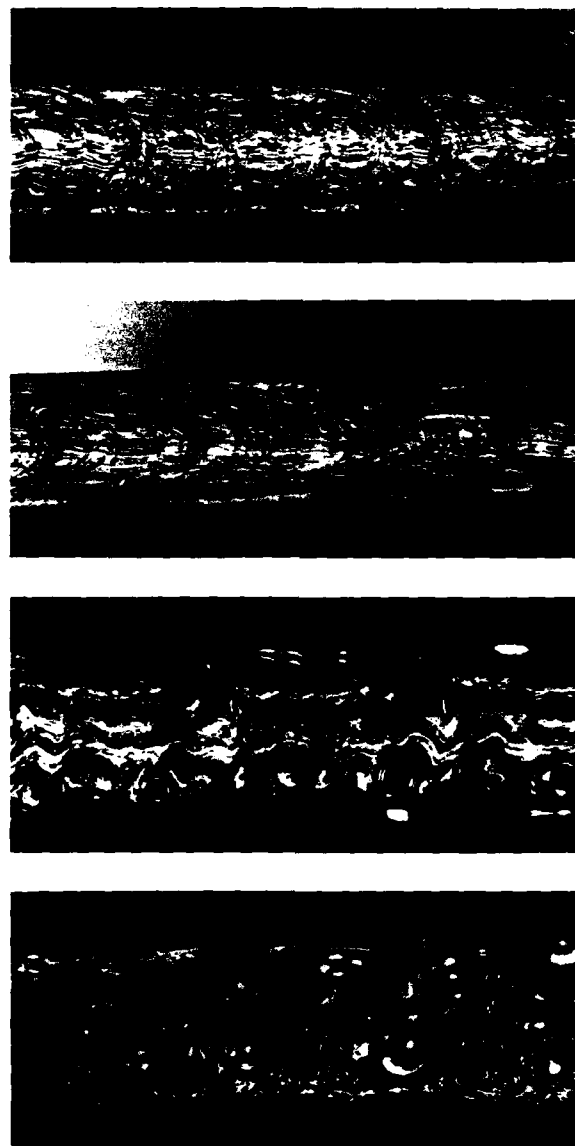
The results of these initial drawing experiments indicate that sound rods can be produced, that the preferred orientation (as judged qualitatively by polarized-light microscopy) is superior to rods produced by extrusion alone,<sup>27</sup> and that the microstructures approach the fine fibrous morphologies desired. However, the extrusion of satisfactory rods is seriously limited by the



1000  $\mu\text{m}$



Fig. 17. Microstructure of a Sound Mesophase Rod Extruded below 340°C.  
Crossed polarizers.



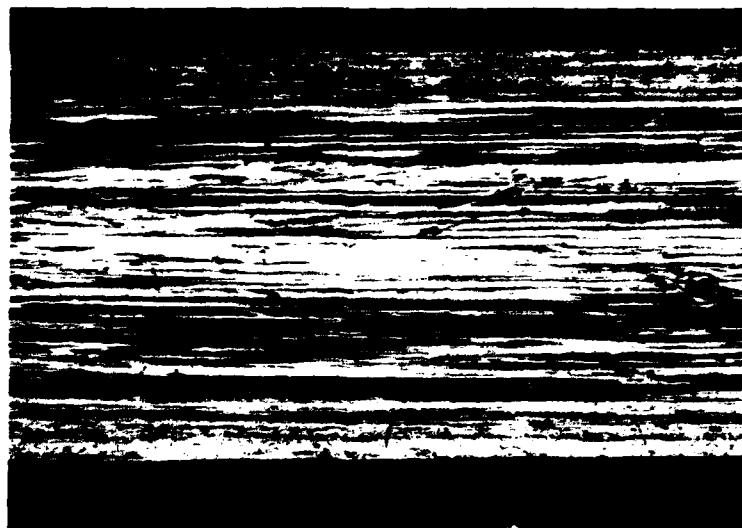
200  $\mu\text{m}$

Fig. 18. Effect of Bubbles in Disrupting the Preferred Orientation of Extruded Mesophase Rods. Extrusion orifice, 200  $\mu\text{m}$ ; crossed polarizers.



1 mm

Fig. 19. Effect of Drawing in Reorienting a Strongly Bubbled Mesophase Rod. Extrusion orifice, 2 mm; crossed polarizers.



500  $\mu\text{m}$



Fig. 20. Microstructure of a Sound Mesophase Rod Produced by Extrusion and Drawing

problem of bubble formation, and we have not yet successfully defined extrusion conditions for the present mesophase pitch that will reproducibly form sound rods for drawing. It may be desirable to explore other mesophase pitches, using the same petroleum pitch but treated to different levels of pyrolysis.

## V. FURTHER INVESTIGATIONS

Further studies of the formation of mesophase microstructures within carbon-carbon composites can be grouped into three tasks: exploration of the effects of pressure up to 15,000 psi, extension of the observations to 3D preforms, and mesophase formation in multiple impregnations. The studies of specimens pyrolyzed at high pressure should be facilitated by the improvement in the autoclave furnace and by the apparent similarities in behavior of both fibers and pitches. The latter generalization will be tested further by including additional varieties of fiber and pitch in the pyrolysis runs. The studies with 3D preforms will focus on the role of the weave cavity in subsequent impregnations as well as in the initial impregnation.

An immediate task in the investigations of mesophase hardening is to define the effect of confining pressure in increasing the pyrolysis intensity required for effective hardening. Another task of basic interest is to correlate the softening point for mechanical deformation with the temperature at which microstructural coarsening begins, e.g., by disclination reactions. Thus our interest in mesophase hardening relates not only to the retention of mesophase in place, as within a preform during pyrolysis, but also to the retention of a microstructure that may have been produced by deformation, as in extrusion or drawing.

Two lines of effort are required to prepare mesophase specimens satisfactory for measurements of heat-treatment effects on dimensions, thermal expansivity, and mechanical properties. First, the variables affecting mesophase extrusion and draw must be further investigated to identify conditions for the reproducible preparation of sound rods consistent in size and microstructure. To overcome the problem of bubbles occurring in the extrudate, it will probably be necessary to prepare a wider variety of mesophase pitches. Second, stabilization processes, operating either by vacuum treatment or by limited oxidation, must be applied to fix the mesophase microstructures before subjecting them to heat treatment.

## VI. REPORTS, PUBLICATIONS, AND PRESENTATIONS

The following list includes reports, publications, and presentations that were completed or are being prepared with support from this research program. Items 11 to 15 are closely related publications and presentations supported by the U.S. Air Force Space Division.

1. J. E. Zimmer and J. L. White, "Disclination Structures in the Carbonaceous Mesophase," Adv. Liq. Cryst. 5, 157-213 (1982); invited review.
2. J. L. White, C. B. Ng, P. M. Sheaffer, and M. Buechler, Mesophase Behavior in Carbon Fiber Bundles, TR-0082(2728-01)-1, The Aerospace Corporation, El Segundo, Calif. (1 June 1982).
3. J. E. Zimmer and J. L. White, "Mesophase Alignment within Carbon Fiber Bundles," Carbon 21, 323-324 (1983).
4. J. L. White, C. B. Ng, G. W. Henderson, and M. Buechler, "Structural Characteristics of Mesophase Carbon Fiber," Extended Abstract for AFWAL/ONR Workshop on Matrix Properties in Carbon-Carbon Composites, Monterey, California, 12-13 May 1982.
5. J. L. White, "Mesophase Mechanisms in Graphite Formation," Ext. Abstr., Int. Symp. Carbon, Toyohashi, Japan (November 1982), pp. 149-152 (invited paper).
6. J. L. White, Mesophase Behavior Fundamental to the Processing of Carbon-Carbon Composites, TR-0083(3728-01)-1, The Aerospace Corporation, El Segundo, Calif. (December 1982); interim technical report on this program for 1 October 1981 through 30 September 1982.
7. J. L. White, P. M. Sheaffer, C. B. Ng, and M. Buechler, "Mesophase Formation within Carbon Fiber Bundles," Ext. Abstr., 16th Conf. Carbon, (1983), pp. 90-91.
8. J. L. White, "Carbon Research and Development in Japan," Sci. Bull., ONR Far East 9, 32-44 (1984).
9. G. W. Smith, J. L. White, and M. Buechler, "Mesophase-Pitch Interfacial Energy Determined from Coalescence Kinetics," Carbon (in press).
10. J. L. White and M. Buechler, "Mesophase Mechanisms in the Formation of Graphite Microstructures," Preprints, Div. of Petroleum Chem., Am. Chem. Soc., 29, 388-397 (1984).

11. J. L. White, M. Buechler, and C. B. Ng, "Microscopic Observations on the Carbonaceous Mesophase by Means of a Quenching Hot Stage," Carbon 20, 536-538 (1982).
12. M. Buechler, C. B. Ng, and J. L. White, "Observations of Mesophase Behavior by a Quenching Hot-Stage Microscope," Ext. Abstr., Int. Symp. Carbon, Toyohashi, Japan (November 1982), p. 143.
13. M. Buechler, C. B. Ng, and J. L. White, "Nonequilibrium Disclinations in the Carbonaceous Mesophase," Carbon 21, 603-605 (1983); also presented, Ext. Abstr., 16th Conf. Carbon (1983), pp. 88-89.
14. C. B. Ng, G. W. Henderson, M. Buechler, and J. L. White, "Fracture Behavior of Mesophase Carbon Fiber," Ext. Abstr., 16th Conf. Carbon, (1983), pp. 515-516.
15. J. L. White, "Carbon Fibers for Large Space Structures," presented to Pacific Coast Regional Meeting of the Am. Ceramic Soc., October 1983.

## REFERENCES

1. J. D. Brooks and G. H. Taylor, Carbon **3**, 185 (1965).
2. J. D. Brooks and G. H. Taylor, Chem. Phys. Carbon **4**, 243 (1968).
3. J. L. White, Prog. Solid State Chem. **9**, 59 (1975).
4. H. Marsh and P. L. Walker, Jr., Chem. Phys. Carbon **15**, 229 (1979).
5. J. L. White, Ext. Abstr., Int. Symp. Carbon, Toyohashi, Japan (1982), p. 149.
6. J. L. White, C. B. Ng, P. M. Sheaffer, and M. Buechler, TR-0082(2728-01)-1, The Aerospace Corporation, El Segundo, Calif. (1 June 1982).
7. J. L. White, TR-0083(3728-01)-1, The Aerospace Corporation, El Segundo, Calif. (December 1982).
8. J. E. Zimmer and J. L. White, Carbon **21**, 323 (1983).
9. J. L. White, P. M. Sheaffer, C. B. Ng, and M. Buechler, Ext. Abstr., 16th Conf. Carbon (1983), p. 90.
10. G. W. Smith, J. L. White, and M. Buechler, Carbon (in press).
11. J. L. White and R. J. Price, Carbon **12**, 321 (1974).
12. J. L. White, in Petroleum Derived Carbons, Am. Chem. Soc. Symp. Series **21**, 282 (1976).
13. J. H. Cranmer, I. G. Plotzker, L. H. Peebles, Jr., and D. R. Uhlmann, Carbon **21**, 201 (1983).
14. V. L. Weinberg and J. L. White, TR-0082(2935-02)-1, The Aerospace Corporation, El Segundo, Calif. (15 December 1981).
15. I. Mochida, M. Z. Wang, Y. Korai, and K. Tamaru, Ext. Abstr., 16th Conf. Carbon (1983), p. 576.
16. J. S. Evangelides and R. A. Meyer, TR-0084(4645-02)-1, The Aerospace Corporation, El Segundo, Calif. (in preparation).
17. J. L. White, M. Buechler, and C. B. Ng, Carbon **20**, 536 (1982).
18. J. Frenkel, J. Phys. (Moscow) **9**, 385 (1945).
19. J. E. Zimmer and R. L. Weitz, Ext. Abstr., 16th Conf. Carbon, 92 (1983).

20. J. B. Barr, S. Chwastiak, R. Didchenko, I. C. Lewis, R. T. Lewis, and L. S. Singer, Appl. Polymer Symp. 29, 161 (1976).
21. G. W. Collett and B. Rand, Fuel 57, 162 (1978).
22. R. Balduhn and E. Fitzer, Carbon 18, 155 (1980).
23. J. C. Jenkins and G. M. Jenkins, Carbon 21, 473 (1983).
24. S. Chwastiak, U. S. Patent 4,209,500 (24 June 1980).
25. R. Didchenko, AFML-TR-73-147, Part I, Report by Union Carbide for Air Force Materials Laboratory (June 1973).
26. F. F. Nazem, Fuel 59, 851 (1980).
27. D. M. Riggs, Ph.D. Dissertation, Rensselaer Polytechnic Institute, Troy, New York (1979).

## LABORATORY OPERATIONS

The Laboratory Operations of The Aerospace Corporation is conducting experimental and theoretical investigations necessary for the evaluation and application of scientific advances to new military space systems. Versatility and flexibility have been developed to a high degree by the laboratory personnel in dealing with the many problems encountered in the nation's rapidly developing space systems. Expertise in the latest scientific developments is vital to the accomplishment of tasks related to these problems. The laboratories that contribute to this research are:

Aerophysics Laboratory: Launch vehicle and reentry fluid mechanics, heat transfer and flight dynamics; chemical and electric propulsion, propellant chemistry, environmental hazards, trace detection; spacecraft structural mechanics, contamination, thermal and structural control; high temperature thermomechanics, gas kinetics and radiation; cw and pulsed laser development including chemical kinetics, spectroscopy, optical resonators, beam control, atmospheric propagation, laser effects and countermeasures.

Chemistry and Physics Laboratory: Atmospheric chemical reactions, atmospheric optics, light scattering, state-specific chemical reactions and radiation transport in rocket plumes, applied laser spectroscopy, laser chemistry, laser optoelectronics, solar cell physics, battery electrochemistry, space vacuum and radiation effects on materials, lubrication and surface phenomena, thermionic emission, photosensitive materials and detectors, atomic frequency standards, and environmental chemistry.

Computer Science Laboratory: Program verification, program translation, performance-sensitive system design, distributed architectures for spaceborne computers, fault-tolerant computer systems, artificial intelligence and microelectronics applications.

Electronics Research Laboratory: Microelectronics, GaAs low noise and power devices, semiconductor lasers, electromagnetic and optical propagation phenomena, quantum electronics, laser communications, lidar, and electro-optics; communication sciences, applied electronics, semiconductor crystal and device physics, radiometric imaging; millimeter wave, microwave technology, and RF systems research.

Materials Sciences Laboratory: Development of new materials: metal matrix composites, polymers, and new forms of carbon; nondestructive evaluation, component failure analysis and reliability; fracture mechanics and stress corrosion; analysis and evaluation of materials at cryogenic and elevated temperatures as well as in space and enemy-induced environments.

Space Sciences Laboratory: Magnetospheric, auroral and cosmic ray physics, wave-particle interactions, magnetospheric plasma waves; atmospheric and ionospheric physics, density and composition of the upper atmosphere, remote sensing using atmospheric radiation; solar physics, infrared astronomy, infrared signature analysis; effects of solar activity, magnetic storms and nuclear explosions on the earth's atmosphere, ionosphere and magnetosphere; effects of electromagnetic and particulate radiations on space systems; space instrumentation.

**END**

**FILMED**

**11-85**

**DTIC**